Linear interaction approximation for shock/disturbance interaction in a Noble–Abel stiffened gas

G. Farag, P. Boivin, P. Sagaut

Linear Interaction Approximation for shock/disturbance interaction in a Noble-Abel stiffened gas

G. Farag[1*], P. Boivin[2] and P. Sagaut[2]

[1]Institut PPRIME - UPR 3346, CNRS - ISAE-ENSMA - Université de Poitiers, Téléport 2, 1 Av. Clément Ader, Chasseneuil-du-Poitou, 86360, France.

[2]Aix Marseille Univ, CNRS, Centrale Marseille, M2P2 UMR 7340, Marseille, France.

*Corresponding author(s). E-mail(s): gabriel.farag@ensma.fr;
Contributing authors: pierre.boivin@univ-amu.fr;
pierre.sagaut@univ-amu.fr;

Abstract

When departure from the ideal gas equation of state is considered, the Noble-Abel stiffened gas model is an appealing and versatile candidate due to its simple form. The Linear Interaction Approximation formalism is extended to consider non-ideal gas effects introduced by this equation of state. Kovásznay decomposition and adequate definition of the energy of disturbances are provided in the context of this equation of state. Changes with respect to ideal gas are investigated on transfer functions, critical angle and compression factor. Those differences yield concrete effects on the damping and transfer of fluctuations across shock waves. Those changes are further illustrated by considering the interaction of an entropy spot with a Mach 3 stationary shock wave.

Keywords: Linear Interaction Approximation, Noble-Abel, Stiffened gas, Shock wave

1 Introduction

This is a preprint version. The published version is available at https://doi.org/10.1007/s00193-023-01131-8

The Linear Interaction Approximation (LIA) for shock/disturbance analysis has been proved to be a very powerful and accurate tool to investigate the physics of the interaction between a shock wave and both laminar and turbulent fluctuating fields [1]. Based on the pioneering works carried out in the 1950s [2, 3], LIA has been progressively extended to more and more complex cases, e.g. mixture of ideal gas [4] and reactive flows [5–8]. A unified framework was recently proposed by [9], along with a mathematically consistent definition of disturbance energy. The extension to non-ideal gas was recently investigated by [10, 11] who proposed fully general relationships for arbitrary equations of state (EOS), with some emphasis put on the BZT dense gas case. For such a complex EOS, some terms can not be computed analytically and must be evaluated numerically. The goal of the present paper is to further work on the extension of LIA for non-ideal gas, by providing a fully explicit theory for the Noble-Abel Stiffened Gas (NASG) model in which all Jacobians are analytically computed.

The paper is organized as follows. Governing equations for an inviscid NASG-type fluid are given in Section 2 along with analytical solution of the 2D Rankine-Hugoniot jump relations for a planar normal shock. Then, the decomposition of both upstream and downstream fluctuating fields for the NASG EOS are discussed in Section 3, followed by the formulation of the LIA problem and Chu's fluctuation energy extension to NASG EOS in Section 4. The physics for the shock/disturbance interaction is investigated considering an upstream Gaussian entropy spot in Section 5. Conclusion is presented in Section 6.

2 Governing equations for the NASG model

We consider here an inviscid fluid, with associated Euler conservation laws supplemented by the NASG EOS proposed by [12], linking the pressure p, mass volume ρ and temperature T as

$$p = \frac{\rho(\gamma-1)C_v T}{1-b\rho} - p_\infty, \tag{1}$$

with C_v the mass heat capacity and $\gamma = C_p/C_v$, the heat capacity ratio. In this EOS, two empirical constants are meant to account for departure from ideal gases, they are b the covolume and p_∞ a reference pressure, respectively accounting for repulsive and attractive effects between molecules. For such a fluid, one has

$$e = \frac{p+\gamma p_\infty}{p+p_\infty} C_v T, \tag{2}$$

for the internal energy, $h = C_p T + bp$ for the enthalpy, $s = C_v \ln T^\gamma/(p+p_\infty)^{\gamma-1}$ for entropy, while the sound velocity c is defined by

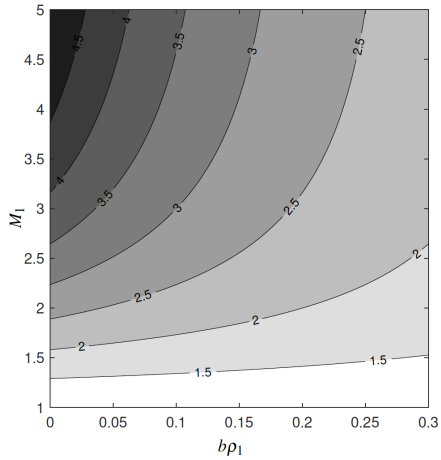

Fig. 1 Compression factor m as function of the upstream shock Mach numer M_1 and the parameter $b\rho_1$.

$$c^2 = \gamma \frac{p + p_\infty}{\rho(1 - b\rho)}. \tag{3}$$

Note that the NASG formulation allows to encompass at once the Clausius-Clapeyron (with $p_\infty = 0$), Stiffened-gas (with $b = 0$) and ideal gas (with $b = p_\infty = 0$) equations of states, thus covering a wide range of applications from gas to liquid and even solid materials, see *e.g.* [13–17].

The closed form analytical framework for modeling compressible flow in a medium approximated by the NASG EOS is given by [18, 19]. In what follows, we briefly recall necessary equations for our purpose. The two-dimensional Rankine-Hugoniot jump conditions for a planar normal shock wave have the following analytical solution :

$$M_2^2 = \frac{2 + (\gamma - 1)M_1^2}{1 + \gamma(2M_1^2 - 1)}, \quad \frac{p_2 + p_\infty}{p_1 + p_\infty} = 1 + \frac{2\gamma}{\gamma + 1}(M_1^2 - 1), \tag{4}$$

where subscripts 1 and 2 are related to upstream and downstream states, respectively, while the compression factor $m = \rho_2/\rho_1 = u_1/u_2$ is given by

$$m = \frac{(\gamma + 1)M_1^2}{2b\rho_1(M_1^2 - 1) + [2 + (\gamma - 1)M_1^2]}, \tag{5}$$

with $M_{1/2}$ the upstream/downstream Mach number. The compression factor m is plotted in Figures 1 in the $(M_1, b\rho_1)$ plane to illustrate the specific features of the NASG fluids with respect to the ideal gas case. We see here that the compression factor m becomes more sensitive to b as the upstream shock Mach number M_1 is increased. This is physically consistent because the molecular repulsive effects modeled by b should be more important for highly compressed materials corresponding to large shock Mach numbers.

For other quantities like temperature and enthalpy, the classical solutions expressed as a function of m hold using the new expression (5). Note that $0 \leq b\rho_1 < 1$ automatically ensures that $0 \leq b\rho_2 < 1$.

3 Kovásznay modal decomposition

The linearized Euler equations for small disturbances about a uniform base flow approximated by the NASG model are

$$\frac{\partial \rho'}{\partial t} + \bar{u}\frac{\partial \rho'}{\partial x} + \bar{\rho}\frac{\partial u'_j}{\partial x_j} = 0, \tag{6}$$

$$\frac{\partial u'_i}{\partial t} + \bar{u}\frac{\partial u'_i}{\partial x} + \frac{1}{\bar{\rho}}\frac{\partial p'}{\partial x_i} = 0, \quad i = 1,2 \tag{7}$$

$$\frac{\partial T'}{\partial t} + \bar{u}\frac{\partial T'}{\partial x} + \frac{\bar{p}+p_\infty}{\bar{\rho}C_v}\frac{\partial u'_j}{\partial x_j} = 0, \tag{8}$$

$$\frac{T'}{\bar{T}} - \frac{p'}{\bar{p}+p_\infty} + \frac{1}{1-b\bar{\rho}}\frac{\rho'}{\bar{\rho}} = 0, \tag{9}$$

$$\frac{s'}{C_p} - \frac{1}{\gamma}\frac{p'}{\bar{p}+p_\infty} + \frac{1}{1-b\bar{\rho}}\frac{\rho'}{\bar{\rho}} = 0, \tag{10}$$

which allow to identify evolution equations for fluctuating entropy, vorticity and pressure as

$$\frac{\partial s'}{\partial t} + \bar{u}\frac{\partial s'}{\partial x} = 0, \tag{11}$$

$$\frac{\partial \omega'}{\partial t} + \bar{u}\frac{\partial \omega'}{\partial x} = 0, \tag{12}$$

$$\left(\frac{\partial}{\partial t} + \bar{u}\frac{\partial}{\partial x}\right)^2 p' = \bar{c}^2\nabla^2 p'. \tag{13}$$

These equations lead to a straight-forward identification of Kovásznay's modes, namely the entropy mode, the vorticity mode and the fast and slow acoustic modes as in the ideal gas case [20, 21].

Now considering plane wave solutions like $\phi' = A_{\mathrm{i}}(\mathbf{k})\exp\left[\mathrm{i}(\mathbf{k}\cdot\mathbf{x} - \Omega t)\right]$ (where ϕ is a dummy variable and subscripts s, v, a are related to entropy mode, vorticity mode and acoustic mode, respectively), the expression given in [9] for the upstream and downstream fluctuating fields are extended as

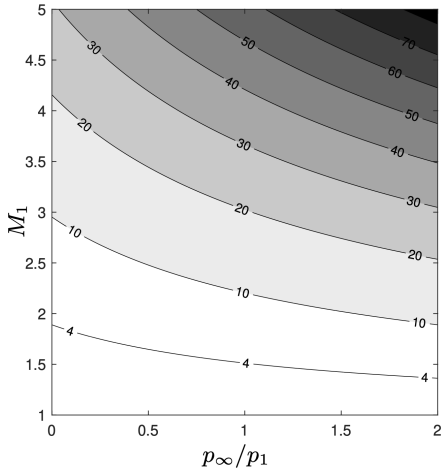

Fig. 2 Critical angle α_c as function of the upstream shock Mach numer M_1 and the parameter $b\rho_1$

$$\begin{bmatrix} \tau_1'/(\bar{\tau}_1 - b) \\ u_1'/\bar{u}_1 \\ v_1'/\bar{u}_1 \\ p_1'/[\gamma(\bar{p}_1 + p_\infty)] \\ T_1'/\bar{T}_1 \\ s_1'/C_{p1} \end{bmatrix} = A_{\mathrm{i}}(\mathbf{k}) \mathrm{e}^{\mathrm{i}(\mathbf{k}\cdot\mathbf{x} - \Omega t)} \begin{bmatrix} \delta_{\mathrm{is}} \\ \delta_{\mathrm{iv}} \sin\alpha \\ -\delta_{\mathrm{iv}} \cos\alpha \\ 0 \\ \delta_{\mathrm{is}} \\ \delta_{\mathrm{is}} \end{bmatrix}, \tag{14}$$

with $\tau = 1/\rho$ and α the incident angle. Formal expressions of the wave numbers of the emitted non-acoustic and acoustic modes, $\mathbf{k}_{\mathrm{s}}$ and $\mathbf{k}_{\mathrm{a}}$, and the critical angle α_c, and the angles of emitted non-acoustic and acoustic modes, α_{s} and α_{a}, and the damping coefficient for emitted evanescent acoustic waves η are identical to those given by [9], but the modified expression of the speed of sound in NASG fluids must be taken into account in the present case.

The critical angle α_c responsible for evanescent waves in the emitted field (see [9] for a detailed definition) can be seen on Figures 2.

It is observed that increasing $b\rho_1$ always results in a decrease of the critical angle, and therefore a decrease in the intensity of emitted fields compared to the ideal gas case. These emitted fluctuating fields are,

$$\begin{bmatrix} \tau_2'/(\bar{\tau}_2 - b) \\ u_2'/\bar{u}_2 \\ v_2'/\bar{u}_2 \\ p_2'/[\gamma(\bar{p}_2 + p_\infty)] \\ T_2'/\bar{T}_2 \\ s_2'/C_{p2} \end{bmatrix} = \begin{bmatrix} -Z_{\mathrm{ia}} \\ Z_{\mathrm{ia}} D_2(\cos\alpha_{\mathrm{a}} + \mathrm{i}\eta)/(M_2\zeta) \\ Z_{\mathrm{ia}} D_2 \sin\alpha_{\mathrm{a}}/(M_2\zeta) \\ Z_{\mathrm{ia}} \\ (\gamma - 1) Z_{\mathrm{ia}} \\ 0 \end{bmatrix}$$

$$\times A_{\mathrm{i}}(\mathbf{k})\mathrm{e}^{-k_{\mathrm{a}}\eta x}\mathrm{e}^{\mathrm{i}(\mathbf{k}_{\mathrm{a}}\cdot\mathbf{x}-\Omega t)}+\begin{bmatrix} Z_{\mathrm{is}} \\ Z_{\mathrm{iv}}\sin\alpha_{\mathrm{s}} \\ -Z_{\mathrm{iv}}\cos\alpha_{\mathrm{s}} \\ 0 \\ Z_{\mathrm{is}} \\ Z_{\mathrm{is}} \end{bmatrix} A_{\mathrm{i}}(\mathbf{k})\mathrm{e}^{\mathrm{i}(\mathbf{k}_{\mathrm{s}}\cdot\mathbf{x}-\Omega t)}, \tag{15}$$

where $\zeta=\sqrt{1-\eta^2+2\mathrm{i}\eta\cos\alpha_{\mathrm{a}}}$ and $D_i=1-b\bar{\rho}_i$. A_{i} denotes the complex amplitude of the upstream mode i and Z_{i} denotes the transfer function between the upstream mode i and the downstream mode j.

4 Formulation of the normal-mode-based LIA

The LIA problem for the evaluation of the complex transfer functions is found in the usual way [1, 22], i.e. considering an upstream-fluctuation-enslaved shock corrugation of the form $x_{\mathrm{s}}(y,t)=A_x\mathrm{e}^{\mathrm{i}(k\sin\beta y-\Omega t)}$ that yields the following linearized jump relation in the base-shock reference frame, which can be expressed as the following linear system for complex transfer functions [1, 9, 22]:

$$\mathrm{M}Z_{\mathrm{i}}=\mathrm{B}_{\mathrm{i}}. \tag{16}$$

In this system we identify the generic matrix M,

$$\mathrm{M}=\begin{pmatrix} \sin\alpha_{\mathrm{s}} & -D_2 & D_2(1+\frac{\cos\alpha_{\mathrm{a}}+\mathrm{i}\eta}{M_2\zeta}) & \mathrm{i}(m-1)\cos\alpha \\ 2\sin\alpha_{\mathrm{s}} & -D_2 & D_2(\frac{M_2^2+1}{M_2^2}+2\frac{\cos\alpha_{\mathrm{a}}+\mathrm{i}\eta}{M_2\zeta}) & 0 \\ -\cos\alpha_{\mathrm{s}} & 0 & D_2(\frac{\sin\alpha_{\mathrm{a}}}{M_2\zeta}) & \mathrm{i}(1-m)\sin\alpha \\ \sin\alpha_{\mathrm{s}} & \frac{D_2^2}{(\gamma-1)M_2^2} & D_2(\frac{1}{M_2^2}+\frac{\cos\alpha_{\mathrm{a}}+\mathrm{i}\eta}{M_2\zeta}) & \mathrm{i}m(1-m)\cos\alpha \end{pmatrix}, \tag{17}$$

the unknown transfer function vector,

$$Z_{\mathrm{i}}=(Z_{\mathrm{iv}},Z_{\mathrm{is}},Z_{\mathrm{ia}},Z_{\mathrm{ix}})^T \tag{18}$$

and the right-hand term, which is dependent on the incident wave's nature,

$$\mathrm{B}_{\mathrm{s}}=\begin{pmatrix} -D_1 \\ -mD_1 \\ 0 \\ \frac{m^2D_1^2}{(\gamma-1)M_1^2} \end{pmatrix},\quad \mathrm{B}_{\mathrm{v}}=\begin{pmatrix} \sin\alpha \\ 2m\sin\alpha \\ -m\cos\alpha \\ m^2\sin\alpha \end{pmatrix}. \tag{19}$$

Differences in the transfer functions between the ideal gas and the NASG EOS for the case $(M_1=3, b\rho_1=0.1)$ are illustrated in Figure 3. Some striking differences are observed. They mainly occur near the critical angle, where we can see that the sharp extrema observed for an ideal gas are highly smoothed by a non-zero covolume

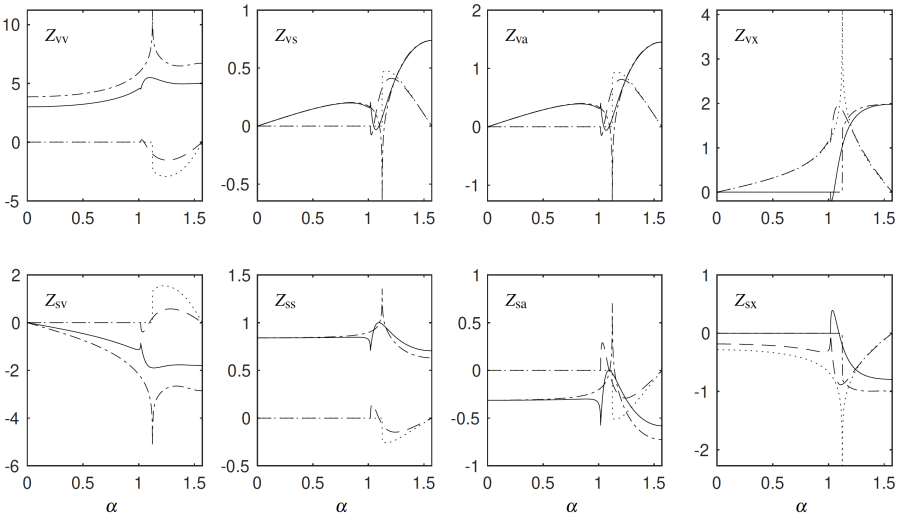

Fig. 3 $b\rho_1 = 0.1$: real part (solid line), imaginary part (dashed) and $b\rho_1 = 0$: real part (dotted-dashed), imaginary part (dotted) of Z_i as a function of the incident wave angle $\alpha \in [0, \pi/2]$, for $\gamma = 1.4$ and $M_1 = 3$.

parameter b. A similar tendency is found for other values of M_1 and $b\rho_1$. On the other hand, the reference pressure does not appears in the LIA system (16) and therefore transfer functions remain independent from p_∞.

The associated definition of the energy of the fluctuating fields derived by [9, 23] based on Chu's seminal work [24] is extended for a NASG EOS as follows:

$$\widetilde{E}_{tot}(t) = \frac{1}{2}\int_V \left\{ \bar{M}^2 \frac{u'^2 + v'^2}{\bar{u}} + \bar{D}^2 \left(\frac{p'}{\gamma(\bar{p} + p_\infty)} \right)^2 + \frac{\bar{D}^2}{\gamma - 1} \left(\frac{s'}{C_p} \right)^2 \right\} \mathrm{d}V. \qquad (20)$$

5 Gaussian entropy spot/shock interaction

To illustrate qualitative effects introduced by the NASG EOS compared to an ideal gas, a parametric study is presented hereafter by considering the interaction between a shock wave and a Gaussian entropy spot at $M_1 = 3$. The upstream disturbance is defined as in [9, 22], i.e. $s' = A_s \mathrm{e}^{-r^2}$ in a spot-centered frame of reference.

The emitted entropy, vorticity and acoustic pressure field are displayed for $b\bar{\rho}_1 = 0$ (ideal gas) and $b\bar{\rho}_1 = 0.1$ in Fig. 4.

The observed reduction of the compression factor m and critical angle α_c in the NASG gas results here in a less anisotropic and more dispersed emitted field with a similar topology when compared to the ideal gas case. Additionally, the normalized emitted modal and total energies are investigated in the $(M_1, b\bar{\rho}_1)$ plane in Fig. 5, the case $M_1 = 3$ being further illustrated in Fig. 6.

As deduced from the variations of the compression factor, the energy of all emitted modes is a decreasing function of $b\bar{\rho}_1$ and an increasing function of M_1. The emitted entropy mode carries almost all the radiated energy, and the damping of the

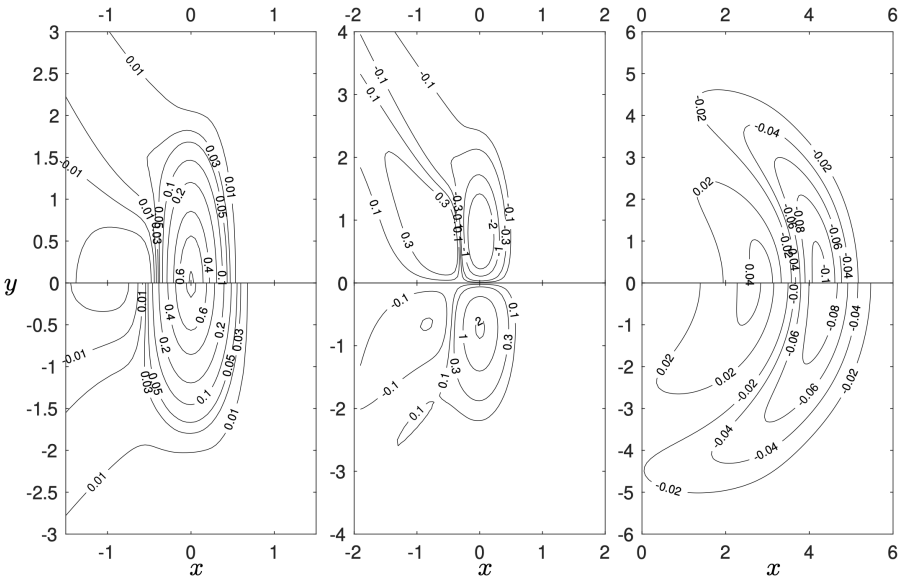

Fig. 4 Incident entropy spot, $M_1 = 3$. From left to right : emitted entropy field, emitted vorticity field, emitted acoustic pressure field. Top sublots : $b\rho_1 = 0$, bottom subplots : $b\rho_1 = 0.1$.

vorticity mode by real gas effects is seen to be more important than for the entropy and acoustic modes.

6 Concluding remarks

The Linear Interaction Approximation has been extended to account for non-ideal thermodynamic effects introduced by the Noble-Abel Stiffened gas EOS [12, 25]. This model encompasses both the Clausius-Clapeyron EOS – valid for high-pressure gases, and the Stiffened gas EOS – commonly adopted when considering high-pressure liquids or solids, allowing to extend the Linear Interaction Approximation theory over a wide range of conditions.

Kovásznay modal decomposition and Chu's energy accounting for the extra parameters introduced by the NASG EOS were proposed. Similar modifications were found in the definition of the orthogonal basis through which the energy of the fluctuating fields [24] is defined. The main non-ideal gas effects found are a decrease of both the critical angle related to evanescent waves and amplitude of the emitted fields when the covolume b is increased.

When considering the NASG EOS $p = \dfrac{\rho(\gamma-1)C_vT}{1-b\rho} - p_\infty$, we found that the p_∞ parameter accounting for attraction forces in high-pressure liquids and solids has a limited effect: only the pressure scaling and the propagation velocity are affected. Using the proper non-dimensional quantities, emitted entropy, vorticity and acoustic pressure fields remain unchanged for incident gaussian spots with varying p_∞.

The covolume b, however, was found to modify the critical and compression factors dependence on the upstream Mach number, and consequently the transfer

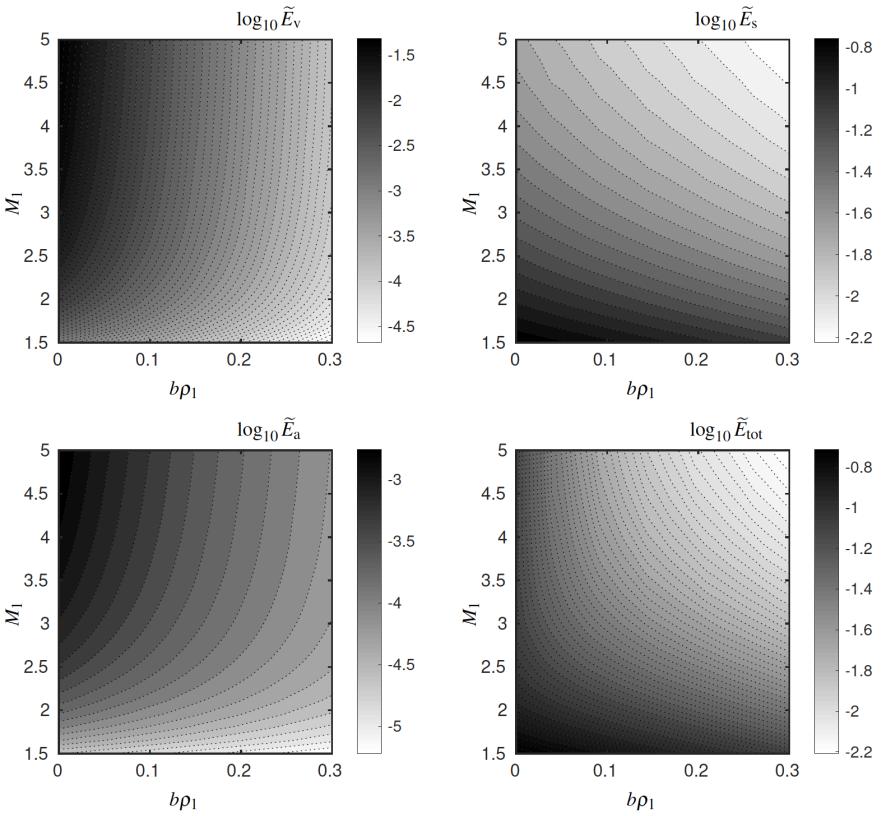

Fig. 5 Energy of the emitted disturbances for an incident Gaussian entropy spot in the $(M_1, b\rho_1)$ plane. Total energy $\widetilde{E}_{tot}$ and the part associated to each Kovásznay mode are displayed, with $\widetilde{E}_{\rm v}$: energy of the vorticity mode; $\widetilde{E}_{\rm a}$: energy of the acoustic mode; $\widetilde{E}_{\rm s}$: energy of the entropy mode.

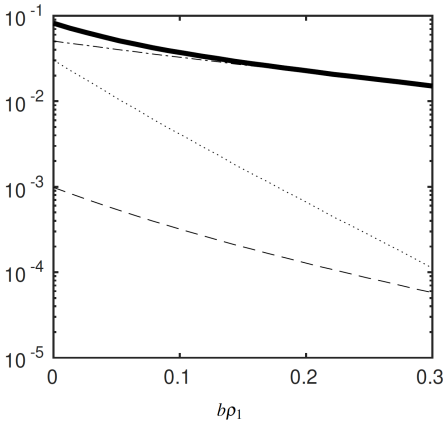

Fig. 6 Energy of the emitted disturbances for a Gaussian entropy spot versus $b\rho_1$ for $M_1 = 3$. Total energy and the part associated to each Kovásznay mode are displayed. $\widetilde{E}_{tot}$ (solid thick line), $\widetilde{E}_{\rm v}$ (dotted), $\widetilde{E}_{\rm a}$ (dashed), $\widetilde{E}_{\rm s}$ (dotted-dashed).

functions through the shock. As a result, entropy incident gaussian spots generate more damped and dispersed emitted fluctuations.

Besides extending our understanding of shock perturbation theory, this work provides interesting test cases for the development of compressible flow solvers with real gas EOS.

Data availability

The datasets generated during and/or analysed during the current study are available from the corresponding author on reasonable request.

Acknowledgements

This work was supported by Labex MEC (ANR-10-LABX-0092) and the A*MIDEX project (ANR-11-IDEX-0001-02), funded by the 'Investissements d'Avenir'.

References

[1] Sagaut, P., Cambon, C.: Homogeneous turbulence dynamics, 2nd edition. Springer Cham (2018). https://doi.org/10.1007/978-3-319-73162-9

[2] Ribner, H.S.: Shock-turbulence interaction and the generation of noise. NACA Technical Note **3255** (1954)

[3] Moore, F.K.: Unsteady oblique interaction of a shock wave with a plane disturbance (1953)

[4] Griffond, J.: Linear interaction analysis applied to a mixture of two perfect gases. Physics of Fluids **17**(8), 086101 (2005). https://doi.org/10.1063/1.1997982

[5] Jackson, T.L., Kapila, A.K., Hussaini, M.Y.: Convection of a pattern of vorticity through a reacting shock wave. Physics of Fluids A: Fluid Dynamics **2**(7), 1260–1268 (1990). https://doi.org/10.1063/1.857626

[6] Jackson, T., Hussaini, M., Ribner, H.: Interaction of turbulence with a detonation wave. Physics of Fluids A: Fluid Dynamics **5**(3), 745–749 (1993). https://doi.org/10.1063/1.858657

[7] Huete, C., Sánchez, A.L., Williams, F.A.: Theory of interactions of thin strong detonations with turbulent gases. Physics of Fluids **25**(7), 076105 (2013). https://doi.org/10.1063/1.4816353

[8] Huete, C., Sánchez, A.L., Williams, F.A.: Linear theory for the interaction of small-scale turbulence with overdriven detonations. Physics of Fluids **26**(11), 116101 (2014). https://doi.org/10.1063/1.4901190

[9] Farag, G., Boivin, P., Sagaut, P.: Interaction of two-dimensional spots with a heat releasing/absorbing shock wave: linear interaction approximation results. Journal of Fluid Mechanics **871**, 865–895 (2019). https://doi.org/10.1017/jfm.2019.324

[10] Alferez, N., Touber, E.: One-dimensional refraction properties of compression shocks in non-ideal gases. Journal of Fluid Mechanics **814**, 185–221 (2017). https://doi.org/10.1017/jfm.2017.10

[11] Touber, E., Alferez, N.: Shock-induced energy conversion of entropy in non-ideal fluids. Journal of Fluid Mechanics **864**, 807–847 (2019). https://doi.org/10.1017/jfm.2019.25

[12] Le Métayer, O., Saurel, R.: The noble-abel stiffened-gas equation of state. Physics of Fluids (1994-present) **28**(4), 046102 (2016). https://doi.org/10.1063/1.4945981

[13] Saurel, R., Le Martelot, S., Tosello, R., Lapébie, E.: Symmetric model of compressible granular mixtures with permeable interfaces. Physics of Fluids **26**(12), 123304 (2014). https://doi.org/10.1063/1.4903259

[14] Chiapolino, A., Boivin, P., Saurel, R.: A simple and fast phase transition relaxation solver for compressible multicomponent two-phase flows. Computers & Fluids **150**, 31–45 (2017). https://doi.org/10.1016/j.compfluid.2017.03.022

[15] Furfaro, D., Saurel, R., David, L., Beauchamp, F.: Towards sodium combustion modeling with liquid water. Journal of Computational Physics **403**, 109060 (2020). https://doi.org/10.1016/j.jcp.2019.109060

[16] Taileb, S., Melguizo-Gavilanes, J., Chinnayya, A.: The influence of the equation of state on the cellular structure of gaseous detonations. Physics of Fluids **33**(3), 036105 (2021). https://doi.org/10.1063/5.0040723

[17] Favrie, N., Schmidmayer, K., Massoni, J.: A multiphase irreversible-compaction model for granular-porous materials. Continuum Mechanics and Thermodynamics **34**(1), 217–241 (2022). https://doi.org/10.1007/s00161-021-01054-8

[18] Radulescu, M.: On the noble-abel stiffened-gas equation of state. Physics of Fluids **31**(11), 111702 (2019). https://doi.org/10.1063/1.5129139

[19] Radulescu, M.I.: Compressible flow in a noble–abel stiffened gas fluid. Physics of Fluids **32**(5), 056101 (2020). https://doi.org/10.1063/1.5143428

[20] Kovasznay, L.S.G.: Turbulence in supersonic flow. Journal of the Aeronautical Sciences **20**(10), 657–674 (1953). https://doi.org/10.2514/8.2793

[21] Chu, B.-T., Kovásznay, L.S.: Non-linear interactions in a viscous heat-conducting compressible gas. Journal of Fluid Mechanics **3**(5), 494–514 (1958). https://doi.org/10.1017/S0022112058000148

[22] Fabre, D., Jacquin, L., Sesterhenn, J.: Linear interaction of a cylindrical entropy spot with a shock. Physics of Fluids **13**(8), 2403–2422 (2001). https://doi.org/10.1063/1.1383592

[23] George, K.J., Sujith, R.: On chu's disturbance energy. Journal of Sound and Vibration **330**(22), 5280–5291 (2011). https://doi.org/10.1016/j.jsv.2011.06.016

[24] Chu, B.-T.: On the energy transfer to small disturbances in fluid flow (part i). Acta Mechanica **1**(3), 215–234 (1965). https://doi.org/10.1007/BF01387235

[25] Boivin, P., Cannac, M., Le Métayer, O.: A thermodynamic closure for the simulation of multiphase reactive flows. International Journal of Thermal Sciences **137**, 640–649 (2019). https://doi.org/10.1016/j.ijthermalsci.2018.10.034